Probing the Dynamics of a Superradiant Quantum Phase Transition with a Single Trapped Ion

Ricardo Puebla, Myung-Joong Hwang, Jorge Casanova, and Martin B. Plenio
Institut für Theoretische Physik and IQST, Albert-Einstein-Allee 11, Universität Ulm, D-89069 Ulm, Germany
(Received 28 July 2016; revised manuscript received 10 January 2017; published 17 February 2017)

We demonstrate that the quantum phase transition (QPT) of the Rabi model and critical dynamics near the QPT can be probed in the setup of a single trapped ion. We first demonstrate that there exists equilibrium and nonequilibrium scaling functions of the Rabi model by finding a proper rescaling of the system parameters and observables, and show that those scaling functions are representative of the universality class to which the Rabi model belongs. We then propose a scheme that can faithfully realize the Rabi model in the limit of a large ratio of the effective atomic transition frequency to the oscillator frequency using a single trapped ion and, therefore, the QPT. It is demonstrated that the predicted universal functions can indeed be observed based on our scheme. Finally, the effects of realistic noise sources on probing the universal functions in experiments are examined.

DOI: 10.1103/PhysRevLett.118.073001

Introduction.—The experimental realization of quantum phase transition (QPT) in a well-controlled quantum system is of considerable interest [1–9]. This is particularly important for the study of the dynamics of QPT where a controlled change of the system parameters is necessary [10–12]. Understanding the dynamics of QPT is at the frontier of the study of critical phenomena; the full extent of the universality in nonequilibrium dynamics of a system that undergoes a QPT remains to be determined [13,14] and its theoretical underpinnings are being actively investigated [15–20].

Trapped ions are a particularly promising platform for this purpose thanks to the possibility of precise coherent quantum control and high-fidelity measurements [3–5], as exemplified by the recent observation of the dynamics of classical phase transitions [21,22]. A major challenge, however, lies in the fact that the QPT typically occurs in a thermodynamic limit where the number of system constituents diverges [23]. Although the universality manifests itself even for a system of finite size in the form of finite-size scaling relations [24–26], it emerges only when the system size is sufficiently large; moreover, a controlled change in the system size under otherwise unchanged conditions is necessary in order to observe the critical exponents. In this respect, and despite the advances in trapped-ion technologies, it is still a formidable challenge to scale up the system size sufficiently to observe critical phenomena while maintaining the controllability and the coherence [5].

Recently, it has been shown in Refs. [20,27] that even a single two-level atom coupled to a harmonic oscillator may undergo a second-order QPT. The experimental realization of such a finite-system QPT is highly desirable, as it opens a possibility to study the dynamics of QPT in a small, fully controlled quantum system with a high degree of coherence without the necessity of scaling the number of system components. However, the required parameter regime [20,27] that includes simultaneously extremely large detuning [28–30] and large coupling strength [31–33] has made it difficult to find a suitable experimental platform to realize the finite-system QPT.

In this Letter, we demonstrate that the QPT of the Rabi model as well as its dynamics can be experimentally observed with a *single* trapped ion whose electronic and vibrational degrees of freedom can be controlled by external radiation. We first demonstrate the existence of a scaling function for the atomic population of the ground state and a nonequilibrium scaling function for the adiabatic dynamics that goes beyond a power-law behavior predicted by the Kibble-Zurek mechanism [10–12,20]. The universality of equilibrium and nonequilibrium scaling functions [17,34] found here is demonstrated by showing that the Dicke model also leads to the identical scaling functions. This result not only corroborates the observation [20] that the Rabi, Dicke [35–37] and Lipkin-Meshkov-Glick [38,39] models may belong to the same universality class [34], but it also extends the universality to the dynamics, too.

Then we consider a concrete trapped-ion realization where the Rabi model is realized by dichromatic sideband lasers such that the atom-coupling strength can be modulated by the intensity of the lasers while the atomic and oscillator frequency can be chosen by the frequency of the lasers [40,41]. However, we show that, in the limit of our interest where the critical behavior emerges, the standard approach based on traveling-wave lasers [40,41] cannot faithfully realize the Rabi model and obscures its universal behavior. We propose and analyze a standing-wave configuration [42,43] including current experimental limitations and show that, when the Rabi frequencies of the lasers

are adiabatically changed, it is indeed possible to observe the universal functions predicted in the first part of the Letter in a realistic trapped-ion setup.

Finally, we examine the effect of different noise sources in our proposal. It is shown that the nonequilibrium universal function is noise resilient thanks to the short adiabatic evolution time that is required, while the equilibrium universal function is largely affected by the noise and requires a long coherence time of the system to be observed.

Finite-frequency scaling.—The Rabi Hamiltonian reads

$$H_{\mathrm{Rabi}} = \omega_0 a^\dagger a + \frac{\Omega}{2}\sigma_z - \lambda(a + a^\dagger)\sigma_x, \tag{1}$$

where $\sigma_{x,z}$ are the Pauli matrices for a two-level atom and a ($a^\dagger$) is an annihilation (creation) operator for a cavity field. The oscillator frequency is ω_0, the atomic transition frequency Ω, and the coupling strength λ. We introduce a dimensionless coupling constant $g = 2\lambda/\sqrt{\omega_0\Omega}$ and the frequency ratio $R = \Omega/\omega_0$. In the $R \to \infty$ limit, the Rabi model undergoes a second-order QPT at the critical point $g = 1$ [20]. For large but not infinite R, the ground state expectation values and the energy spectrum exhibit a critical scaling in R at $g = 1$, so-called *finite-frequency* scaling [20]. Here we focus on the ground state population of the two-level atom $\langle\sigma_z\rangle$ because it is possible to measure it with high fidelity in the trapped-ion system [44,45], and we derive the analytic expression for its scaling relations.

In the $R \to \infty$ limit we have $\langle\sigma_z\rangle = -1$ for $g \le 1$ and $\langle\sigma_z\rangle = -(1/g^2)$ for $g > 1$ [20]. Its singular part is $\langle\sigma_z\rangle_s \equiv \langle\sigma_z\rangle + 1 = (1 - g^{-2})$ vanishing as $\langle\sigma_z\rangle_s \propto (g-1)^\gamma$ near the critical point with a critical exponent $\gamma = 1$. We now consider $\langle\sigma_z\rangle_s$ as a function of R and g, denoted by $\langle\sigma_z\rangle_s(R, g)$, and examine specifically its scaling behavior for finite R. Particularly, we find the analytical expression of the finite-frequency scaling for $R \gg 1$ and $g = 1$ as

$$\langle\sigma_z\rangle_s(R, g = 1) \propto R^{-\mu}, \tag{2}$$

where $\mu = 2/3$ is the finite-frequency scaling exponent of σ_z. See the Supplemental Material [46] for the derivation of Eq. (2). Furthermore, by a rescaling of the expectation value and coupling strength as

$$S_s \equiv |g-1|^{-\gamma}\langle\sigma_z\rangle_s, \qquad G \equiv R|g-1|^{\gamma/\mu}, \tag{3}$$

we find that the ground state population of the spin can be cast into a function $S_s(G)$, called the scaling function [24–26]. The functional form can be obtained by (i) calculating $\langle\sigma_z\rangle_s(R, g)$ with the numerically exact diagonalization for different values of R and g satisfying $R \gg 1$ and $|g-1| \ll 1$ and (ii) plotting the rescaled quantity $S_s = |g-1|^{-\gamma}\langle\sigma_z\rangle_s$ as a function of $G = R|g-1|^{\gamma/\mu}$. As shown in Fig. 1(a), the data points collapse onto a single curve, which confirms the existence and reveals the functional form of $S_s(G)$. We also find an analytic expression for the asymptotic behavior of $S_s(G)$ as $\lim_{G\to 0} S_s(G) \propto G^{-\mu}$, which agrees very well with the numerical results [Fig. 1(a)]. We emphasize that the scaling function $S_s(G)$ and the dynamical scaling function, to be introduced below, are universal functions in that another model, e.g., the Dicke model, shows the same scaling functions [46].

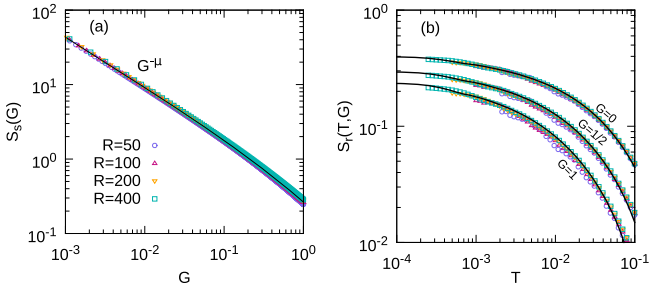

FIG. 1. Universal functions of the Rabi model. (a) Rescaled ground state population $S_s(G)$ as a function of $G = R|g-1|^{\gamma/\mu}$, with $\gamma = 1$ and $\mu = 2/3$, for different frequency ratio $R = 50$, 100, 200, and 400 and coupling strength $0.9 \le g \le 1$. For $G \ll 1$, it follows a power law $S_s(G) \propto G^{-\mu}$. (b) Rescaled residual atomic population $S_r(T, G)$ as a function of $T = R^{-1}\tau_q$ for a fixed value of the rescaled final coupling strength $G_f = R|g_f - 1|^{\gamma/\mu} = 0$, $1/2$, and 1. The quench time τ_q varies from $0.1/\omega_0$ to $100/\omega_0$ and $0.9 \le g_f \le 1$. The same values of R as in (a) have been used.

Adiabatic evolution and dynamical scaling.—We now consider the adiabatic dynamics of the Rabi model. To this end, we prepare an initial state $|\Psi(t=0)\rangle = |0\rangle|\downarrow\rangle$, where $|0\rangle$ is the zero phonon Fock state and $|\downarrow\rangle$ is an atomic eigenstate, and increase the coupling strength linearly in time from $g_i = 0$ to g_f for a duration τ_q; that is, $g(t) = g_f t/\tau_q$. For large enough τ_q to satisfy the adiabatic condition [47], one can prepare the ground state of the Rabi model with $g = g_f$ for a fixed R to high fidelity and measure σ_z to observe the ground state universal function $S_s(G)$ and the scaling exponent μ discussed in the previous section. A potential limit to this approach is that the spectral gap Δ vanishes at the QPT ($R \to \infty$) as $\Delta \propto |g-1|^\zeta$, where $\zeta = 1/2$ [20,23], and, for a finite R, the gap Δ of H_{Rabi} decays as a power law $\Delta \propto R^{-\mu\zeta/\gamma} = R^{-1/3}$ near the critical point; therefore, for $R \gg 1$, the adiabatic condition requires τ_q to be much larger than the coherence time of the system. While we examine the feasibility of the adiabatic preparation in the last section, here we consider the case when τ_q becomes progressively smaller; then, the adiabatic condition starts to break down near the critical point first, while it is still satisfied away from it. In other words, we go beyond the equilibrium setting and examine the universality in adiabatic dynamics of the QPT.

The key insight is that, because of the equilibrium critical scaling, e.g., shown in Eq. (2), one can cast the equation of motion for the adiabatic evolution into a universal form through a rescaling of parameters [17–19]. For the Rabi model, we find that by rescaling the evolution time τ_q as

$T \equiv R^{-\gamma/\mu(1+\zeta)}\tau_q$, where $\gamma/\mu(1+\zeta)=1$, and together with the rescaling of the coupling strength $G = R|g-1|^{\gamma/\mu}$ introduced in Eq. (3), the equation of motion transforms into a universal form [46], which does not depend individually on R, g, or τ_q. The central quantity of our interest is again σ_z. Let us denote $\langle\sigma_z\rangle_f(R, g_f, \tau_q)$ as the expectation value of σ_z for the final state of the adiabatic evolution for a given τ_q at the final coupling strength g_f and the frequency ratio R, and $\langle\sigma_z\rangle(R, g_f)$ as the ground state expectation value for a given R and $g = g_f$. Now we introduce the residual atomic population $\langle\sigma_z\rangle_r(R, g_f, \tau_q) \equiv |\langle\sigma_z\rangle_f(R, g_f, \tau_q) - \langle\sigma_z\rangle(R, g_f)|$, which quantifies the nonadiabaticity of the evolution and vanishes for a τ_q satisfying the adiabatic condition. Our main result is that the rescaled residual atomic population $S_r \equiv R^{\mu}\langle\sigma_z\rangle_r$ is a universal function of the rescaled parameters T and G [46]. To confirm this prediction, we solve the dynamics for different τ_q and calculate $\langle\sigma_z\rangle_r$ for a set of values of g_f and R leading to a fixed value of $G_f = R|g_f - 1|^{\gamma/\mu}$. Then, we plot S_r as a function of T and show that all the data points with the same value of G_f collapse into a single curve, confirming that $S_r(T, G_f)$ is a universal function [Fig. 1(b)]. It is clear that different choices of G_f lead to different universal curves, as S_r is a function of both G_f and T.

Trapped-ion realization.—We consider a setup of a single trapped ion with two traveling-wave lasers, described by $H_{\rm TI}(t) = \nu a^\dagger a + (\omega_I/2)\sigma_z + \sum_{j=1,2}(\Omega_j^d/2)\times \sigma_+ e^{i[\eta_j(a+a^\dagger)-\omega_j^d t-\phi_j^d]} + \text{H.c.}$, where $a(\sigma_-)$ is an annihilation operator for a phonon (internal levels). The phonon frequency is ν and the transition frequency ω_I. For the jth laser, ω_j^d is the frequency, ϕ_j^d the phase, Ω_j^d the Rabi frequency, and $\eta_j = k_j\sqrt{1/(2m\nu)}$ is the Lamb-Dicke parameter, with k_j being the wave vector and m the ion mass. We consider two driving frequencies near the blue- and red-sideband transitions, respectively; i.e., $\omega_{1,2}^d = \omega_I \mp \nu + \delta_{1,2}$, where $\delta_{1,2} \ll \nu$ are additional detunings with respect to each sideband and we set $\Omega_{1,2}^d = \Omega^d$, $\eta_{1,2} = \eta$, and $\phi_{1,2}^d = 3\pi/2$. Note that the so-called optical rotating-wave approximation (RWA) has already been made to $H_{\rm TI}(t)$, which is well known to hold in this setting.

In a rotating frame with respect to $H_{\rm TI}^0 = (\nu - \tilde{\omega}_0)a^\dagger a + \frac{1}{2}(\omega_I - \tilde{\Omega})\sigma_z$, $H_{\rm TI}(t)$ becomes time independent and assumes the form of the Rabi model [40,41]:

$$\tilde{H}_{\rm TI}(t) = e^{-iH_{\rm TI}^0 t}H_{\rm TI}(t)e^{iH_{\rm TI}^0 t} \simeq \tilde{\omega}_0 a^\dagger a + \frac{\tilde{\Omega}}{2}\sigma_z - \tilde{\lambda}(a + a^\dagger)\sigma_x. \tag{4}$$

Here the new set of parameters for the Rabi model is $\tilde{\omega}_0 = \frac{1}{2}(\delta_1 - \delta_2)$, $\tilde{\Omega} = \frac{1}{2}(\delta_1 + \delta_2)$, and $\tilde{\lambda} = \eta\Omega^d/2$. Equation (4) is valid only within the Lamb-Dicke regime, i.e., $\eta\sqrt{\langle(a + a^\dagger)^2\rangle} \ll 1$, and the vibrational RWA; therefore, it is not *a priori* evident that one can probe the QPT of the Rabi model using this approach. The universal properties of the Rabi model emerge when $R = \tilde{\Omega}/\tilde{\omega}_0 \gg 1$ and $g = 2\tilde{\lambda}/\sqrt{\tilde{\omega}_0\tilde{\Omega}} \simeq 1$. However, the phonon population in the ground state monotonically grows as one increases $\tilde{\Omega}/\tilde{\omega}_0$, leading to a potential departure from the Lamb-Dicke regime. Furthermore, the strong coupling strength $\tilde{\lambda} \simeq \sqrt{\tilde{\omega}_0\tilde{\Omega}}$ requires a large Rabi frequency of the laser, which could break the vibrational RWA. Hence, we now need to study in detail whether the desired regime $R \gg 1$ and $g \cong 1$ can indeed be reached.

To this end, we apply the adiabatic protocol discussed in the previous section directly to the trapped-ion Hamiltonian $H_{\rm TI}(t)$ without assuming any simplification, neither the Lamb-Dicke regime nor the vibrational RWA. This involves preparing the initial state $|\Psi(t=0)\rangle = |0\rangle|\downarrow\rangle$, where $|0\rangle$ is the zero-phonon Fock state and $|\downarrow\rangle$ is the low-energy state of the ion, and adiabatically turning on the Rabi frequencies $\Omega^d(t)$ for a duration of τ_q until it reaches the desired final value of $g = g_f$; that is, $\Omega^d(t) = \Omega_f^d t/\tau_q$ with $\Omega_f^d = g_f\sqrt{\delta_1^2 - \delta_2^2}/2\eta$, while the detunings $\delta_{1,2}$ are chosen to realize a fixed value of R and remain fixed during the adiabatic evolution. Then, one measures the σ_z operator of the final states of the adiabatic evolution and finds the universal functions $S_s(G)$ and $S_r(T, G)$, as described in the previous section.

A possible set of achievable parameters for the Rabi model in the trapped ion setup is $\tilde{\omega}_0/2\pi = 200$ Hz and $10 \le \tilde{\Omega}/2\pi \le 80$ kHz, so that the frequency ratios $50 \le R \le 400$ can be explored. This implies that the Rabi frequency at $g = 1$ is $23.6 \le \Omega^d/2\pi \le 66.6$ kHz, where we have used $\eta = 0.06$. For the adiabatic preparation of the ground state, the considered evolution time is $\tau_q = 50/\tilde{\omega}_0 = 250$ ms, which approximately satisfies the adiabatic condition [46]. For the dynamical scaling, one can choose a smaller range, $0.1/\tilde{\omega}_0 \le \tau_q \le 2/\tilde{\omega}_0$, or, equivalently, $0.5 \le \tau_q \le 10$ ms. The numerics with the above parameters [Figs. 2(a) and 2(b)] show a strong deviation from the theoretical prediction of the Rabi model; that is, the rescaled expectation values do not collapse into the predicted universal function.

We identify that a leading-order contribution to the breakdown of Eq. (4) is a carrier interaction, i.e., $-i(\Omega^d/2)(\sigma_+ e^{i\delta_j t} - \sigma_- e^{-i\delta_j t})$ for $j = 1, 2$, that is induced by both sideband transitions due to the large values of Ω^d used to achieve a strong coupling strength $\tilde{\lambda}$. The effect of this process becomes dominant for $R \gg 1$ and obscures the universality of the Rabi model [Figs. 2(a) and 2(b)]. To resolve this issue, we propose to use a standing-wave configuration for the sideband lasers so that the carrier interaction is suppressed. That is, we consider two additional

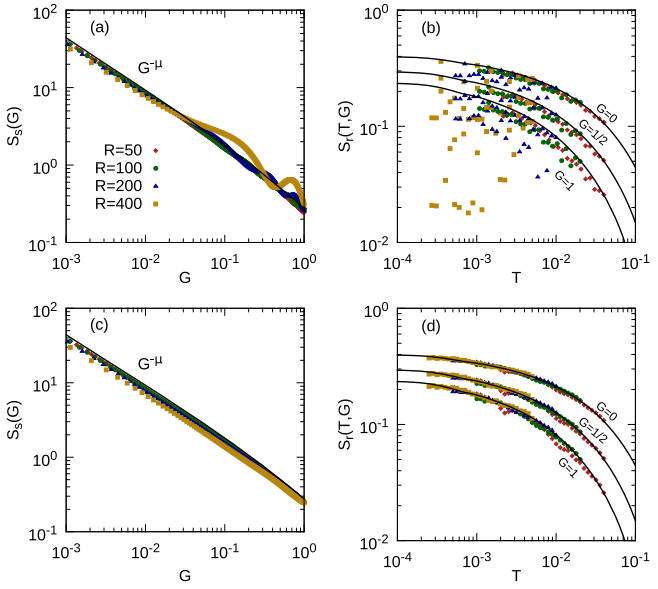

FIG. 2. Universal functions $S_s(G)$ and $S_r(T,G)$ obtained from the trapped-ion Hamiltonians with the scheme of (a),(b) two lasers and (c),(d) four lasers, together with the result presented in Fig. 1 (solid line). The different points represent different R with a fixed effective oscillator frequency $\tilde{\omega}_0/2\pi = 200$ Hz. In (a) and (c), the quench time is $\tau_q = 50/\tilde{\omega}_0 = 250$ ms. In (b) and (d), a range of quench time $0.5 \leq \tau_q \leq 10$ ms for three different values $G = 0$, $1/2$, and 1 is used.

lasers in $H_{\mathrm{TI}}(t)$, labeled as $j = 3, 4$, such that $\omega_3^d = \omega_1^d$ and $\omega_4^d = \omega_2^d$ and $\eta_1 = -\eta_3$ and $\eta_2 = -\eta_4$. The phases are chosen as $\phi_{3,4} = \pi/2$ and the Rabi frequencies of two counterpropagating lasers are ideally identical: $\Omega_{3,4}^d = \Omega_{1,2}^d = \Omega^d$.

In the standing-wave configuration the effective coupling strength is $\tilde{\lambda} = \eta\Omega^d$. Hence, to realize $g = 1$, one needs $11.8 \leq \Omega^d/2\pi \leq 33.3$ kHz, which is a factor of 2 smaller than in the traveling-wave configuration. The numerical results for the standing-wave configuration are presented in Figs. 2(c) and 2(d), which show an excellent agreement with the prediction of the Rabi model [Figs. 2(c) and 2(d)] and demonstrate that it is possible to probe the universal functions of the Rabi model in a trapped-ion setup with the standing-wave configuration. Note that Figs. 2(c) and 2(d) show that experimentally inevitable differences in the Rabi frequencies of the counterpropagating lasers, i.e., $\Omega_{3,4} \neq \Omega_{1,2}$ (up to 8% of error is considered [43]), do not affect the feasibility of the scheme.

Effects of noise.—During the adiabatic evolution various noise sources will have an impact on the final states. Here we examine this impact and demonstrate that the nonequilibrium universal function can be observed under realistic experimental conditions. The master equation that governs the adiabatic evolution is $\dot{\rho} = -i[H_{\mathrm{Rabi}}(t),\rho] + \Gamma_{dp}\mathcal{L}[\sigma_z] + \Gamma_c\mathcal{L}[\sigma_-] + \Gamma_a\mathcal{L}[a] + \Gamma_h\mathcal{L}[a^\dagger]$, where $\mathcal{L}[x] = x\rho x^\dagger - x^\dagger x\rho/2 - \rho x^\dagger x/2$. Typical parameters are $\Gamma_{dp}/2\pi = 20$ Hz and $\Gamma_{c,a,h} = 10$ Hz. Therefore, we set $\Gamma_{dp}/\omega_0 = 0.1$ and $\Gamma_{c,a,h}/\omega_0 = 0.05$ and solve the adiabatic dynamics with the same system parameters used in the previous section.

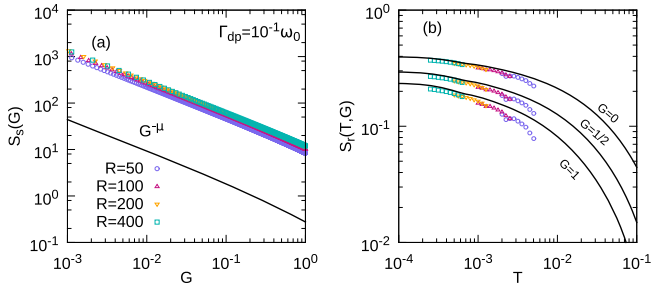

FIG. 3. Effect of noises on the universal functions. The rates $\Gamma_{dp} = 0.1\omega_0$ and $\Gamma_{c,a,h} = 0.05\omega_0$ are used with the same system parameters used in the Fig. 1 to produce the solid line. (a) The graphs corresponding to the different R do not collapse onto the universal curve; see Ref. [46] for a discussion. (b) A rather short range of quench time $0.1/\omega_0 \leq \tau_q \leq 0.275/\omega_0$ is used, as the longer time evolution deviates from the universal behavior due to the effect of noise [46]; while this leads to smaller data points than Figs. 1 and 2, it nevertheless correctly reveals the substantial part of the universal function.

Figure 3(a) shows that $S_s(G)$ is strongly influenced by the noise. For different R, the graphs no longer collapse onto the predicted universal function. This is because the quench time $\tau_q \sim 250$ ms required to meet the adiabatic condition is much longer than the coherence time of 50 ms; therefore, a lower noise rate, $\Gamma_{dp}/\omega_0 \lesssim 10^{-3}$, would be required to its experimental observation [46].

On the other hand, Fig. 3(b) shows that $S_r(T,G)$ is much more robust to the effect of noise, and the universality in the dynamics remains intact. The robustness of the nonequilibrium universal function to noises stems from the relatively short evolution time τ_q compared to the coherence time. While the small spectral gap near the critical point necessitates a very large τ_q for the adiabatic preparation of the ground state, the nearly adiabatic dynamics considered here requires the adiabaticity only away from the critical point where the energy gap does not vanish, which makes its experimental observation more favorable than the equilibrium case.

Conclusions.—We have demonstrated that the Rabi QPT and its universal dynamics can be observed with a single trapped ion that interacts with one of its vibrational modes under realistic experimental conditions. We use the equilibrium and nonequilibrium universal scaling functions as a probe, where the latter is demonstrated to be more robust against experimental noise sources. Our work, therefore, opens the door for experimental exploration of the finite-system quantum phase transition in trapped ion systems.

This work was supported by the Alexander von Humboldt foundation, the ERC Synergy grant BioQ, the EU STREP project EQUAM, and the CRC TRR21.

[1] M. Greiner, O. Mandel, T. Esslinger, T. W. Hänsch, and I. Bloch, Nature (London) **415**, 39 (2002).
[2] I. Bloch, J. Dalibard, and S. Nascimbène, Nat. Phys. **8**, 267 (2012).
[3] D. Porras and J. I. Cirac, Phys. Rev. Lett. **92**, 207901 (2004).
[4] K. Kim, M. S. Chang, S. Korenblit, R. Islam, E. E. Edwards, J. K. Freericks, G. D. Lin, L. M. Duan, and C. Monroe, Nature (London) **465**, 590 (2010).
[5] R. Islam, E. E. Edwards, K. Kim, S. Korenblit, C. Noh, H. Carmichael, G. D. Lin, L. M. Duan, C. C. J. Wang, J. K. Freericks, and C. Monroe, Nat. Commun. **2**, 377 (2011).
[6] A. Bermudez and M. B. Plenio, Phys. Rev. Lett. **109**, 010501 (2012).
[7] K. Baumann, C. Guerlin, F. Brennecke, and T. Esslinger, Nature (London) **464**, 1301 (2010).
[8] F. Dimer, B. Estienne, A. S. Parkins, and H. J. Carmichael, Phys. Rev. A **75**, 013804 (2007).
[9] D. Nagy, G. Kónya, G. Szirmai, and P. Domokos, Phys. Rev. Lett. **104**, 130401 (2010).
[10] B. Damski, Phys. Rev. Lett. **95**, 035701 (2005).
[11] W. H. Zurek, U. Dorner, and P. Zoller, Phys. Rev. Lett. **95**, 105701 (2005).
[12] A. Polkovnikov, Phys. Rev. B **72**, 161201 (2005).
[13] S. Braun, M. Friesdorf, S. S. Hodgman, M. Schreiber, J. P. Ronzheimer, A. Riera, M. del Rey, I. Bloch, J. Eisert, and U. Schneider, Proc. Natl. Acad. Sci. U.S.A. **112**, 3641 (2015).
[14] J. Klinder, H. Keßler, M. Wolke, L. Mathey, and A. Hemmerich, Proc. Natl. Acad. Sci. U.S.A. **112**, 3290 (2015).
[15] A. Polkovnikov, K. Sengupta, A. Silva, and M. Vengalattore, Rev. Mod. Phys. **83**, 863 (2011).
[16] J. Eisert, M. Friesdorf, and C. Gogolin, Nat. Phys. **11**, 124 (2015).
[17] M. Kolodrubetz, B. K. Clark, and D. A. Huse, Phys. Rev. Lett. **109**, 015701 (2012).
[18] G. Nikoghosyan, R. Nigmatullin, and M. B. Plenio, Phys. Rev. Lett. **116**, 080601 (2016).
[19] O. L. Acevedo, L. Quiroga, F. J. Rodríguez, and N. F. Johnson, Phys. Rev. Lett. **112**, 030403 (2014).
[20] M.-J. Hwang, R. Puebla, and M. B. Plenio, Phys. Rev. Lett. **115**, 180404 (2015).
[21] K. Pyka, J. Keller, H. Partner, R. Nigmatullin, T. Burgermeister, D. Meier, K. Kuhlmann, A. Retzker, M. Plenio, W. Zurek *et al.*, Nat. Commun. **4**, 2291 (2013).
[22] S. Ulm, J. Roßnagel, G. Jacob, C. Degünther, S. Dawkins, U. Poschinger, R. Nigmatullin, A. Retzker, M. Plenio, F. Schmidt-Kaler *et al.*, Nat. Commun. **4**, 2290 (2013).
[23] S. Sachdev, *Quantum Phase Transitions*, 2nd ed. (Cambridge University Press, Cambridge, England, 2011).
[24] M. E. Fisher and M. N. Barber, Phys. Rev. Lett. **28**, 1516 (1972).
[25] R. Botet, R. Jullien, and P. Pfeuty, Phys. Rev. Lett. **49**, 478 (1982).
[26] R. Botet and R. Jullien, Phys. Rev. B **28**, 3955 (1983).
[27] M.-J. Hwang and M. B. Plenio, Phys. Rev. Lett. **117**, 123602 (2016).
[28] S. Ashhab, Phys. Rev. A **87**, 013826 (2013).
[29] L. Bakemeier, A. Alvermann, and H. Fehske, Phys. Rev. A **85**, 043821 (2012).
[30] M.-J. Hwang and M.-S. Choi, Phys. Rev. A **82**, 025802 (2010).
[31] J. Bourassa, J. M. Gambetta, A. A. Abdumalikov, O. Astafiev, Y. Nakamura, and A. Blais, Phys. Rev. A **80**, 032109 (2009).
[32] S. Ashhab and F. Nori, Phys. Rev. A **81**, 042311 (2010).
[33] J. Casanova, G. Romero, I. Lizuain, J. J. García-Ripoll, and E. Solano, Phys. Rev. Lett. **105**, 263603 (2010).
[34] H. E. Stanley, Rev. Mod. Phys. **71**, S358 (1999).
[35] K. Hepp and E. H. Lieb, Ann. Phys. (N.Y.) **76**, 360 (1973).
[36] C. Emary and T. Brandes, Phys. Rev. Lett. **90**, 044101 (2003).
[37] J. Vidal and S. Dusuel, Europhys. Lett. **74**, 817 (2006).
[38] S. Dusuel and J. Vidal, Phys. Rev. Lett. **93**, 237204 (2004).
[39] S. Dusuel and J. Vidal, Phys. Rev. B **71**, 224420 (2005).
[40] J. I. Cirac, A. S. Parkins, R. Blatt, and P. Zoller, Phys. Rev. Lett. **70**, 556 (1993).
[41] J. S. Pedernales, I. Lizuain, S. Felicetti, G. Romero, L. Lamata, and E. Solano, Sci. Rep. **5**, 15472 (2015).
[42] J. I. Cirac, R. Blatt, P. Zoller, and W. D. Phillips, Phys. Rev. A **46**, 2668 (1992).
[43] T. E. deLaubenfels, K. A. Burkhardt, G. Vittorini, J. T. Merrill, K. R. Brown, and J. M. Amini, Phys. Rev. A **92**, 061402 (2015).
[44] A. H. Myerson, D. J. Szwer, S. C. Webster, D. T. C. Allcock, M. J. Curtis, G. Imreh, J. A. Sherman, D. N. Stacey, A. M. Steane, and D. M. Lucas, Phys. Rev. Lett. **100**, 200502 (2008).
[45] A. H. Burrell, D. J. Szwer, S. C. Webster, and D. M. Lucas, Phys. Rev. A **81**, 040302 (2010).
[46] See Supplemental Material at http://link.aps.org/supplemental/10.1103/PhysRevLett.118.073001 for further explanation and details of the calculation.
[47] A. Messiah, *Quantum Mechanics* (Dover Publications, New York, 1961).